ISSN (Print) 1226-1750
ISSN (Online) 2233-6656
Journal of Magnetics 18(4), 386-390 (2013) http://dx.doi.org/10.4283/JMAG.2013.18.4.386

Magnetic and Magnetocaloric Properties of Perovskite $Pr_{0.5}Sr_{0.5-x}Ba_xMnO_3$

Sihao Hua, Pengyue Zhang*, Hangfu Yang, Suyin Zhang, and Hongliang Ge

College of Material Science and Engineering, China Jiliang University, Hangzhou 310018, China

(Received 15 May 2013, Received in final form 30 August 2013, Accepted 30 August 2013)

This paper studies the effects of A-site substitution by barium on the magnetic and magnetocaloric properties of $Pr_{0.5}Sr_{0.5-x}Ba_xMnO_3$ (x = 0, 0.04, 0.08 and 0.1). The tetragonal crystal structures of the samples are confirmed by room temperature X-ray diffraction. The dependence of the Curie temperature (T_C) and the magnetic entropy change (ΔS_M) on the Ba doping content has been investigated. The samples of all doping contents undergo the second order phase transition. As the concentration of Ba increased, the maximum entropy change ($|\Delta S_M|_{max}$) increased gradually, from 1.15 J kg^{-1} K^{-1} (x = 0) to 1.36 J kg^{-1} K^{-1} (x = 0.1), in a magnetic field change of 1.5 T. The measured value of T_C is 265 K, 275 K, 260 K and 250 K for x = 0, 0.04, 0.08 and 0.1, respectively. If combining these samples for magnetic refrigeration, the temperature range of ~220 K and 290 K, where $|\Delta S_M|_{max}$ is stable at ~1.27 J kg^{-1} K^{-1} and RCP = 88.9 J·kg^{-1} for ΔH = 1.5 T. $Pr_{0.5}Sr_{0.5-x}Ba_xMnO_3$ compounds, are expected to be suitable for magnetic-refrigeration application due to these magnetic properties.

Keywords : magnetocaloric effect, manganite, magnetic properties, curie temperature

1. Introduction

The magnetic refrigeration based on the magnetocaloric effect (MCE), which is the temperature change of a material arising from the variation of the applied magnetic field, has attracted attention for its significant advantages when compared with the traditional gas-compression technology, with the characteristics of higher energy efficiency and environmental friendliness [1-4]. The working principle of magnetic refrigeration is the MCE, which refers to an isothermal change in the magnetic entropy (ΔS_M) and an adiabatic change in the temperature of the sample (ΔT_{ad}) when the samples are subjected to a changing magnetic field (H). Materials with large MCE have attracted growing interest owing to the possible application as a magnetic refrigerant. For a long time, Gd was considered to be a prime candidate refrigerant for its large magnetic entropy change and the suitable Curie temperature (T_C) around room temperature ($|\Delta S_M|$ = 10.2 J kg^{-1} K^{-1} at ΔH = 5.0 T, T_C = 294 K) [5]. Nonetheless, the commercial application was limited by the expensive price of Gd. The amounting research has explored various new materials with large magnetocaloric effects, such as $LaFe_{11.4}Si_{1.6}$ [6], $Gd_5Si_2Ge_2$ [7], MnFe(P,As) [8] and hole doped perovskite manganites [9]. Perovskite manganites with the general formula $Ln_{1-x}A_xMnO_3$ (Ln = trivalent rare earth, A = divalent alkaline earth) are believed to be good candidates for magnetic refrigeration over various temperature ranges, because its magnetic entropy change (ΔS_M), Curie temperature (T_C) and colossal magnetoresistance effect are strongly doping-dependent. Therefore, more researches regarding the magnetic properties of perovskite manganites have been conducted in recent years [10-12].

The perovskite $Pr_{1-x}Sr_xMnO_3$ was an important member of the manganite family with an intermediate one electron bandwidth [13]. The Pr-based manganites showed many novel properties, such as the charge ordering (CO) state and the coexistence of ferromagnetic (FM) and antiferromagnetic phase (AFM) [14-16]. As for $x < 0.4$ in $Pr_{1-x}Sr_xMnO_3$, it possessed a strong FM-PM phase transition along with a large magnetoresistance effect; for $x \geq 0.5$, it showed a CO-antiferromagnetic state. The large positive ΔS_M results from a field-induced structure transition that accompanied the destruction of the antiferromagnetic. The MCE of manganite $Pr_{0.5}Sr_{0.5}MnO_3$ has been studied for several years, and the giant value of S_M in the polycrystalline manganite of $Pr_{0.5}Sr_{0.5}MnO_3$ was found to be 7.1 J kg^{-1} K^{-1} at 160 K for ΔH = 1.0 T, which is much larger than that of Gd (ΔS_M = –2.8 J kg^{-1} K^{-1} at ΔH = 1.0T) [4]. Nowadays, researchers focus on the doping

*Corresponding author: Tel: +86-186-68006322
Fax: +86-571-28889526, e-mail: zhang_pengyue@cjlu.edu.cn

different elements (K, Na, Ag, Eu, Dy etc.) on A-site in order to get a larger magnetic entropy change as well as to tailor the phase transition temperature. Yang *et al.* [17] have conducted serial experiments about the monovalent metals doped in $Pr_{0.5}Sr_{0.5}MnO_3$, suggesting that the maximum magnetic entropy changes reached 1.8, 2.2, 1.6 and 2.1 J kg^{-1} K^{-1} for Na, Li , K and Ag, respectively; the ΔS_M fits well with the Landau theory of the phase transition above T_C for $Pr_{0.5}Sr_{0.3}Li_{0.2}MnO_3$.

Yu and Phan studied MCE of Ba doped $La_{0.7}Ca_{0.3}MnO_3$, suggesting that the materials exhibit a large magnetic entropy change of $|\Delta S_M|_{max}$ 1.85 J kg^{-1} K^{-1} at 298 K investigated up to 1.0 T [18]. However, few lectures reported the Ba doping in the $Pr_{0.5}Sr_{0.5}MnO_3$. In the present work, we investigated the effect of different doping content of Ba substitution on the structure, the magnetocaloric properties and the Curie temperature of $Pr_{0.5}Sr_{0.5}MnO_3$.

2. Experimental Details

Polycrystalline of $Pr_{0.5}Sr_{0.5-x}Ba_xMnO_3$ (x = 0, 0.04, 0.08 and 0.1) is synthesized by the standard solid state reaction method at high temperature. The starting materials (Pr_6O_{11}, $SrCO_3$, $MnCO_3$, $BaCO_3$) are mixed with stoichiometric quantities and mixed in agate mortar. The mixture is heated in air up to 1273 K for 24 h after ball milling for 2 h. After heated, they are reground, pressed into pellets that are 2 mm in thickness and 13 mm in diameter. Then the pellets are sintered at 1773 K. Finally, these pellets are slowly cooled down to room temperature. The crystal structures of the samples are detected by X-ray diffraction (XRD) at room temperature. Magnetic properties are measured by a vibrating sample magnetometer (VSM Lakeshore 7407) with the magnetic field in the range of 0-1.5 T.

3. Results and Discussion

The X-ray diffraction patterns of the samples are shown in Fig. 1. All the samples are found to be in a single phase crystallize pervoskite structure without any detectable secondary phase. The diffraction peaks are indexed with

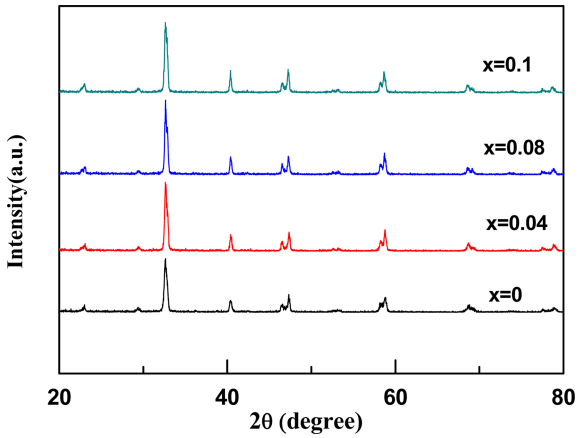

Fig. 1. (Color online) XRD patterns of $Pr_{0.5}Sr_{0.5-x}Ba_xMnO_3$ samples (x = 0, 0.04, 0.08 and 0.1).

respect to the tetragonal structure with a space group of I4/mcm. The characteristic peaks gradually shift to the left, which is associated with large lattice parameters with the increase of the doping content. This indicates that doping with Ba has an influence on the lattice parameters, which is due to the chemical substitution of bigger Ba^{2+} ions (1.42 Å) doping into the smaller Sr^{2+} (1.26 Å) ionic site [19]. The average A-site-cation radius (<r_A>), the *A*-site cationic size mismatch (σ^2) and tolerance factor (*t*), are also shown in Table 1. The <r_A> and σ^2 gradually increase while the content of Ba increases. A characteristic parameter used to describe the manganite behavior is the ionic size tolerance factor (t), defined as:

$$t = \frac{r_A + r_O}{\sqrt{2}(r_B + R_O)},$$

where r_A is the average radius of La-site atoms, r_o is the radius of the O^{2-} ion, and r_B is the average radius of Mn-site atoms. Manganite perovskite can be stable when the value of the tolerance factor places between 0.89 and 1.02. Further, the structure obtains better symmetry properties when the value of the tolerance factor is close to 1 [20]. The increase value of *t* can be used to prove the influence on the structure with Ba doping.

Figure 2 shows the temperature dependence of zero-field cooled magnetization (ZFC) and field cooled magneti-

Table 1. Lattice parameter (a, c), volume (V), average A-site-cation radius <r_A>, tolerance factor (t) and A-site cationic size mismatch (σ^2) in $Pr_{0.5}Sr_{0.5-x}Ba_xMnO_3$.

Nominal composition	a (Å)	c (Å)	V (Å^3)	t	<r_A>	σ^2
$Pr_{0.5}Sr_{0.5}MnO_3$	5.416	7.7916	228.61	0.895	1.193	4.489×10^{-3}
$Pr_{0.5}Sr_{0.46}Ba_{0.04}MnO_3$	5.4201	7.8024	229.22	0.897	1.199	6.329×10^{-3}
$Pr_{0.5}Sr_{0.42}Ba_{0.08}MnO_3$	5.4321	7.7943	229.99	0.899	1.206	8.088×10^{-3}
$Pr_{0.5}Sr_{0.4}Ba_{0.1}MnO_3$	5.4324	7.8019	230.25	0.900	1.209	8.937×10^{-3}

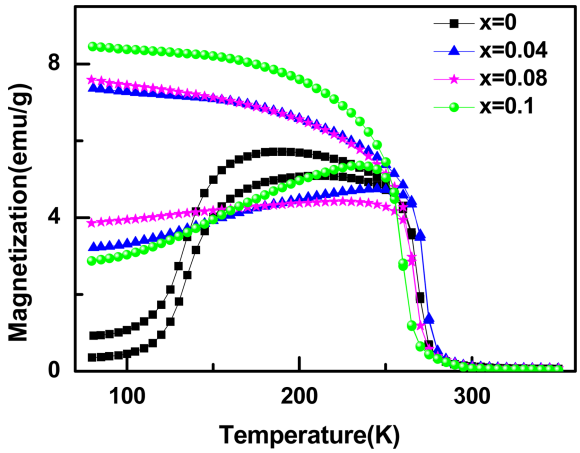

Fig. 2. (Color online) Temperature dependence of zero field cooled (ZFC) and field cooled (FC) magnetization curves measured at 100 Oe for $Pr_{0.5}Sr_{0.5-x}Ba_xMnO_3$ (x = 0, 0.04, 0.08 and 0.1).

zation (FC) with the increase of temperature under H = 0.01 T for $Pr_{0.5}Sr_{0.5-x}Ba_xMnO_3$ (x = 0, 0.04, 0.08 and 0.1). The Curie temperature can be obtained from the critical points of dM/dT in Fig. 2. T_C is calculated to be 265 K, 275 K, 260 K and 250 K for x = 0, 0.04, 0.08 and 0.1, respectively. The value of Curie temperature reaches highest when x = 0.04, and then decreases with the doping content increase. Phan *et al.* reported that Curie temperature increases with the increase of the doping level in $La_{0.7}Ca_{0.3-x}Ba_xMnO_3$ [18]. It can be interpreted that the partial replacement of Ca with Ba can lead to an increase in $<r_A>$. In general, the average A-site ionic radius $<r_A>$ increases, resulting in a change in Mn-O bond length and Mn-O-Mn bond angle. This causes the weakening of the exchange effect. Consequently, the Curie temperature decreases [21]. However, the Curie temperatures drops with $<r_A>$ arising in our work. For x = 0.04, the Curie temperature increases slightly, then with the doping content increase, the Curie temperature gradually decreases. N. Abdelmoula *et al.* [22] interpreted that the exchange energy does not only depend on the Mn^{3+}/Mn^{4+}, but also on the $<r_A>$ of the A site. For x = 0.04, the rise of $<r_A>$ is not the main factor to influence the double exchange effect, and a few doping of Ba change the ratio of Mn^{3+}/Mn^{4+}, which influence the exchange energy. Hence, the slight increase of $<r_A>$ cannot weaken the exchange effect. However, for x = 0.08 and 0.1, the T_C reduces greatly, demonstrating a striking difference to others, which is attributed to the increase of the A-site cationic size mismatch σ^2 (shown in Table 1), weakening the double exchange interaction. Moreover, the increase of $<r_A>$ also becomes an important factor weakening the double exchange effect. These results demonstrate that a reduction of the double exchange interaction energy produces the decrease in the ferromagnetic phase.

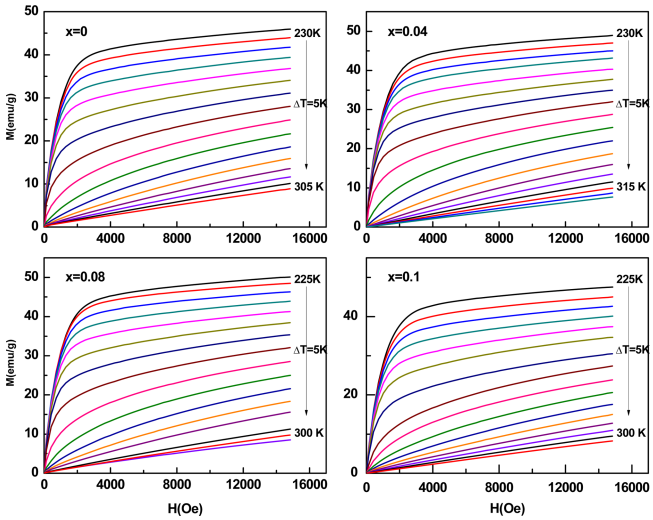

Fig. 3. (Color online) Isothermal magnetization curves of $Pr_{0.5}Sr_{0.5-x}Ba_xMnO_3$ (x = 0, 0.04 and 0.08) at different temperatures.

The isothermal magnetization curves (M-H) of the samples are measured in the magnetic field change of 1.5 T at different temperatures around T_C (Fig. 3). The feature can be divided into two regions. The first region, which is nonlinear, shows the FM phase; and the second linear region is associated with the PM phase. No S-shape curve is found in M-H curves, implying that all samples undergo a second order magnetic phase transition. In order to clearly observe the types of phase transition in $Pr_{0.5}Sr_{0.5-x}Ba_xMnO_3$, we performed Arrott curves of H/M versus M^2, as shown in Fig. 4. The positive slope in all $H/$

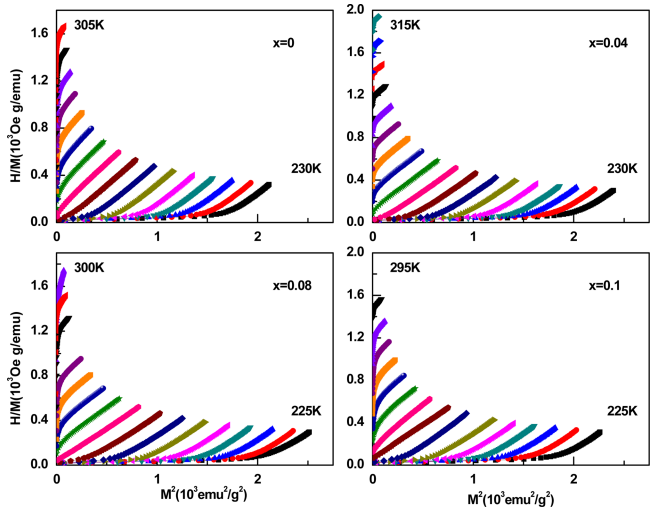

Fig. 4. (Color online) Arrott plots (H/M versus M^2) of $Pr_{0.5}Sr_{0.5-x}Ba_xMnO_3$ (x = 0, 0.04 and 0.08) at different temperatures.

M versus M^2 curves implies that our samples undergo a second order phase transition, according to the Banerjee criterion [30].

From magnetization isotherms, we calculated the total magnetic entropy change $|\Delta S_M|$ as a function of temperature and magnetic applied field for all our synthesized samples. According to the thermodynamic theory based on Maxwell relations, $|\Delta S_M|$ can be evaluated through the formula:

$$\Delta S_M(T, H) = S_M(T, H) - S_M(T, Q) = \int_0^{H_{max}} \left(\frac{\partial M}{\partial T}\right) dH, \quad (1)$$

where H_{max} is the maximum value of the external magnetic applied field. In practice, for magnetization measurement, this relation can be approximated as:

$$|\Delta S_M| = \sum_i \frac{M_i - M_{i+1}}{T_{i+1} - T_i} \Delta H_i, \quad (2)$$

where M_i and M_{i+1} are the experimental values of magnetization measured at temperatures T_i and T_{i+1}, respectively, under a magnetic applied field H_i [23]. ΔS_M can be calculated from the isothermal M-H curves at a series of temperatures by using Eq. (2).

The magnetic entropy change ΔS_M as a function of temperature is obtained by using Eq. (2); thus, the ΔS_M in magnetic field of 1.5 T is shown in Fig. 4. It is found that ΔS_M of $Pr_{0.5}Sr_{0.5}MnO_3$ varies with the temperature and reaches their maximum at the PM-FM transition temperature T_C. The maximum values of ΔS_M are –1.15 J kg^{-1} K^{-1}, –1.24 J kg^{-1} K^{-1}, –1.33 J kg^{-1} K^{-1} and –1.36 J kg^{-1} K^{-1} for x = 0, 0.04, 0.08 and 0.1, respectively. It can be seen that the value of $|\Delta S_M|_{max}$ increases with the increase of the Ba content. The similar behavior was observed in the layered pervoskite manganese oxide $La_{1.4}(Sr_{1-x}Ba_x)_{1.6}Mn_2O_7$ [31]. In this paper, with the development of the Ba content, the magnetization becomes large thereby leading to the increase of $|\Delta S_M|_{max}$. The magnetization of samples can be easily calculated from ZFC and FC curves, showing that the value with x = 0.1 is the largest. Large magnetization generally induces a large magnetic entropy change. Moreover, the spin-lattice coupling in the magnetic ordering process may also play an important role on the large magnetic entropy changes in manganites [24].

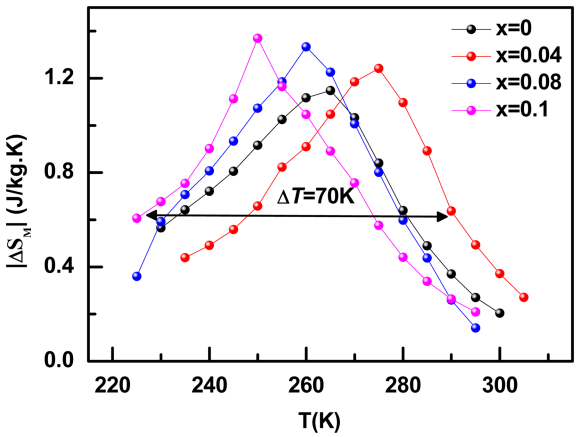

Fig. 5. (Color online) Magnetic entropy change ΔS_M as a function of the temperature for $Pr_{0.5}Sr_{0.5-x}Ba_xMnO_3$ (x = 0, 0.04, 0.08 and 0.1).

To assess the applicability of $Pr_{0.5}Sr_{0.5-x}Ba_xMnO_3$ samples for magnetic refrigeration, the values of $|\Delta S_M|_{max}$ determined in the present studies are compared in Table 2 with those reported in the literature for several materials considered promising for such application.

On the other hand, the cooling efficiency of magnetic refrigerants can be inferred by means of relative cooling power (RCP), which corresponds to the amount of heat transferred between cold and the hot sinks in the refrigeration cycle [25]. The relative cooling power value is defined as RCP = $|\Delta S_M|_{max} \times \delta T_{FWHM}$, where δT_{FWHM} is the width of half the maximum ΔS_M versus the T curve. RCP values estimated for the present set of $Pr_{0.5}Sr_{0.5-x}Ba_xMnO_3$ samples are 59.8, 55.8, 55.9 and 58.5 J·kg^{-1} for x = 0, 0.04, 0.08 and 0.1, respectively. If we pay more attention to ΔS_M curves, it can be found that the width of half the maximum ΔS_M (δT_{FWHM}) decreases from 52 K (for x = 0) to 42 K (for x = 0.1). Zhang *et al.* [26] reported that by combining the samples of $La_{0.7}Ca_{0.3}Mn_{1-x}Co_xO_3$ for the magnetic-refrigeration application, a temperature range can be used between 210 K and 275 K (with ΔT = 65 K). In our case, a temperature range of the combining samples ($Pr_{0.5}Sr_{0.5-x}Ba_xMnO_3$) can be used between 220 K and 290 K (with ΔT = 70 K), which means that the width

Table 2. Magnetic entropy change ($|\Delta S_M|_{max}$) and RCP for several manganites and element Gd in low magnetic field.

Nominal composition	T_C (K)	H (T)	$\|\Delta S_M\|_{max}$ (J·kg^{-1}·K^{-1})	RCP (J·kg^{-1})	Reference
$Pr_{0.64}Sr_{0.36}MnO_3$	320	2.5	2.3	34.5	27
$Pr_{0.55}Sr_{0.45}MnO_3$	291	3.0	1.71	43.6	28
Gd	294	1.5	3.8	–	29
$Pr_{0.5}Sr_{0.3}Ba_{0.08}MnO_3$	260	1.5	1.33	55.8	Present work
$Pr_{0.5}Sr_{0.35}Ba_{0.1}MnO_3$	250	1.5	1.36	58.5	Present work

is wider than that of $La_{0.7}Ca_{0.3}Mn_{1-x}Co_xO_3$.

4. Conclusion

We have studied the structure, the magnetic properties and the magnetocaloric effect of $Pr_{0.5}Sr_{0.5-x}Ba_xMnO_3$ in the tetragonal crystal structure. It is found that the Curie temperature decreases and the magnetic entropy changes gradually increase with the increase of the Ba content, and that the samples are of the second-order phase transition. With the Ba doping, the contents of $<r_A>$ and σ^2 change; hence, the double exchange interaction is weakened, resulting in the decrease of T_C. Compared with MCE of other manganites studied, $Pr_{0.5}Sr_{0.5-x}Ba_xMnO_3$ is expected to be a suitable refrigerant for applications in the temperature range of ~220 K and 290 K, where $|\Delta S_M|_{max}$ is stable at ~1.27 J kg^{-1} K^{-1} and RCP = 88.9 J·kg^{-1} for ΔH = 1.5 T.

Acknowledgments

This work was supported by Project of Zhejiang Province Innovative Research Team (No. 2010R50016), the Provincial Natural Science Foundation (Y6100640) National Natural Science Foundation of China (No. 51001092, 51301158 and 51371163) and National Public Interest Research Special (No. 201210107).

References

[1] V. K. Pecharsky and K. A. Gschneidner, J. Magn. Magn. Mater. **200**, 44 (1999).
[2] K. A. Gschneidner and V. K. Pecharsky, Rep. Prog. Phys. **68**, 1479 (2005).
[3] E. Brück, J. Phys. D **38**, R381 (2005).
[4] M. H. Phan and S. C Yu, J. Magn. Magn. Mater. **308**, 325 (2007).
[5] S. Yu. Dankov, A. M. Tishin, V. K. Pecharsky, and K. A. Gschneidner Jr., Phys. Rev. B **57**, 3478 (1998).
[6] F. X. Hu, B. G. Shen, J. R. Sun, Z. H. Cheng, G. H. Rao, and X. X. Zhang, Appl. Phys. Lett. **78**, 3675 (2001).
[7] V. K. Pecharsky, and K. A. Gschneidner Jr., Appl. Phys. Lett. **70**, 3299 (1997).
[8] O. Tegus, E. Brück, K. H. J. Buschow, and F. R. de Boer, Nature **415**, 150 (2002).
[9] X. X. Zhang, J. Taiada, Y. Xin, G. F. Sunm, K. W. Wong, and X. Bohigas, Appl. Phys. Lett. **69**, 3596 (1996).
[10] A. Szewczyk, H. Szymczak, A. Wisniewski, K. Piotrowski, R. Kartaszynski, B. Dabrowski, S. Kolesnik, and Z. Bukowski, Appl. Phys. Lett. **77**, 1026 (2000).
[11] Y. Sun, X. Xu, and Y. H. Zhang, J. Magn. Magn. Mater. **219**, 183 (2000).
[12] A. Biswas, T. Samanta, S. Benerjee, and I. Das, Appl. Phys. Lett. **94**, 233109 (2009).
[13] E. Pollert, Z. Jirak, J. Hejtmanek, A. Strejc, R. Kuzel, and V. Hardy, J. Magn. Magn. Mater. **246**, 290 (2002).
[14] T. Wu, and M. Mitchell, Phys. Rev. B **69**, 100405(R) (2004).
[15] S. Hebert, A. Maignan, V. Hardy, C. Martin, M. Hervieu, B. Raveau, R. Mahendiran, and P. Schiffer, Eur. Phys. J. B **29**, 419 (2002).
[16] R. Mahandiran, A. Maignan, S. Hebert, C. Martin, M. Hervieu, B. Raveau, J. F. Mitchell, and P. Schiffer, Phys. Rev. Lett. **89**, 286602 (2002).
[17] H. F. Yang, P. Y. Zhang, Q. Wu, H. L. Ge, and M. X. Pan, J. Magn. Magn. Mater. **324**, 3727 (2012).
[18] M-H Phan, S. B. Tian, S. C. Yu, and A. N. Ulyanov, J. Magn. Magn. Mater. **256**, 306 (2003).
[19] R. D. Shannon, Acta Cryst. **32**, 751 (1976).
[20] V. Franco, J. S. Blazquez, B. Ingale, and A. Conde, Mater. Res. **42**, 305 (2012).
[21] J. Dhahri, A. Dhahri, and E. Dhahri, J. Magn. Magn. Mater. **321**, 4128 (2009).
[22] N. Abdelmoula, J. Dhahri, K. Guidara, E. Dhahri, and J. C. Joubert, Phase Tran-sit. **70**, 211 (1999).
[23] M. Moumen, A. Mehri, W. Chikhrouhou-Koubaa, M. Koubaa, and A. Cheikhrouhou, J. Alloys Compd. **509**, 9084 (2011).
[24] Z. B. Guo, Y. W. Du, J. S. Zhu, H. Huang, W. P. Ding, and D. Feng, Phys. Rev. Lett. **78**, 1142 (1997).
[25] K. A. Gschneidner and V. K. Pecharsky, Annu. Rev. Mater. Sci. **30**, 387 (2000).
[26] Y. D. Zhang, The-Long Phan, and S. C. Yu, J. Appl. Phys. **111**, 07D703 (2012).
[27] S. Zemni, M. Baazaoui, Ja. Dhahri, H. Vincent, and M. Oumezzine, Materials Letters. **63**, 489 (2009).
[28] J. Y. Fan, L. Pi, L. Zhang, W. Tong, and L. S. Ling, Physica B **406**, 2289 (2011).
[29] V. K. Pecharsky and K. A. Gschneidner, J. Appl. Phys. **90**, 4614 (2001).
[30] B. K. Banerjee, Phys. Lett. **12**, 16 (1964).
[31] K. Cherif, S. Zemni, J. Dhahri, M. Oumezzine, M. Said, and H. Vincent, J. Alloys Compd. **432**, 30 (2007).